Inorganic Chemistry

ARTICLE

pubs.acs.org/IC

Interaction of Ferrocene Moieties Across a Square Pt_4 Unit: Synthesis, Characterization, and Electrochemical Properties of Carboxylate-Bridged Bimetallic Pt_4Fe_n (n = 2, 3, and 4) Complexes

Shinji Tanaka and Kazushi Mashima*

Department of Chemistry, Graduate School of Engineering Science, Osaka University, and CREST, JST, Toyonaka, Osaka 560-8531, Japan

Supporting Information

ABSTRACT: Four types of square Pt_4 complexes bearing two or more ferrocenecarboxylate ligands—$[Pt_4(\mu\text{-}OCOCH_3)_4(\mu\text{-}OCOC_5H_4FeCp)_4]$ (**6**); $[Pt_4(\mu\text{-}OCOCH_3)_4(\mu\text{-}OCOC_5H_4FeCp)_3(\mu\text{-}ArNCHNAr)]$, where ArNCHNAr = *N*,*N*′-diarylformamidinate) (**7**); *trans*-$[Pt_4(\mu\text{-}OCOCH_3)_4(\mu\text{-}OCOC_5H_4FeCp)_2(\mu\text{-}ArNCHNAr)_2]$ (**8**); and *cis*-$[Pt_4(\mu\text{-}OCOCH_3)_4(\mu\text{-}OCOC_5H_4FeCp)_2(\kappa^4\text{-}N_4\text{-}DArBp)_2]$, where DArBp = 1,3-bis(benzamidinato)propane (**9**)—were successfully prepared via reactions of $[FeCp(\eta^5\text{-}C_5H_4COOH)]$ (**5**) with the corresponding square Pt_4 complexes, which have labile *in-plane* acetate ligands. The newly prepared Pt_4 complexes (**6**−**9**) with ferrocene moieties as pendants were characterized by nuclear magnetic resonance (NMR) spectroscopy, mass spectroscopy (MS), combustion analyses, and single-crystal X-ray analysis for **6**, some of the *trans*-Pt_4Fe_2 **8**, and the *cis*-Pt_4Fe_2 complexes **9**. Weak interactions between two ferrocene moieties across the Pt_4 core, providing $\Delta E_{1/2}$ values and K_c constants, were revealed electrochemically, using cyclic and differential-pulse voltammetry in dichloromethane containing $[^nBu_4N][BAr^F{}_4]$ (where Ar^F = $C_6H_3(CF_3)_2$-3,5), which was a better supporting electrolyte for such an interaction than $[^nBu_4N][PF_6]$.

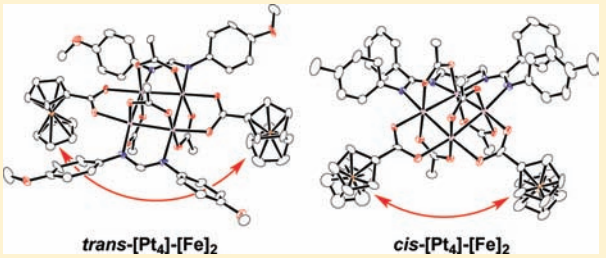

INTRODUCTION

Multimetallic complexes have recently attracted much attention, because of their peculiar redox properties, magnetism, and catalytic applications, which are due to the cooperative effects of their multimetallic centers.[1−7] Among these intrinsic trends, multimetallic complexes assembled with redox active units are of particular interest, in terms of their multielectron systems and unique electron transfer events through the multimetallic core.[8−10] Ferrocene and its derivatives are widely utilized for these purposes, because of their chemical stability, synthetic versatility, and reversible one-electron redox behavior;[11,12] yet, there are only limited examples of multimetallic complexes capped and/or connected by ferrocene pendants and/or spacers.[13−21] Accordingly, the electrochemistry of multiferrocene units through multimetallic complexes was anticipated to show distinct interactions between Fe centers.[16b,e,18b,21]

We have been investigating the use of a tetraplatinum complex, $[Pt_4(\mu\text{-}OCOCH_3)_8]$ (**1**; see Chart 1)[22,23] as a multimetallic core, which has a square tetraplatinum skeleton supported by four *in-plane* acetate ligands and four *out-plane* acetate ones, because four *in-plane* acetate ligands can be selectively substituted by organic ligands such as carboxylates, diamines, pyridine, etc.[24] We have already succeeded in synthesizing three types of Pt_4 complexes: *trans*-$[Pt_4(\mu\text{-}OCOCH_3)_6(\mu\text{-}ArNCHNAr)_2]$ (**2**), $[Pt_4(\mu\text{-}OCOCH_3)_7(\mu\text{-}ArNCHNAr)]$ (**3**), and *cis*-$[Pt_4(\mu\text{-}OCOCH_3)_6(\kappa^4\text{-}N_4\text{-}DArBp)]$, where DArBp = *N*,*N*′-bis(arylformamidinato)propane) (**4**) (see Chart 1). These three complexes serve as units for the rational construction of a supramolecular array, and we also have elucidated their electronic properties.[25] Herein, we report the synthesis of four types of Pt_4−ferrocenecarboxylate complexes, in which the number and positions of ferrocenecarboxylate ligands attached to the Pt_4 core were controlled by treating the Pt_4 complexes (**1**−**4**) with a ferrocenecarboxylic acid $[FeCp(\eta^5\text{-}C_5H_4COOH)]$ (**5**),[13c,14,17,18,19a,26] and we reveal weak interactions of the ferrocene moieties across the square Pt_4 unit based on electrochemical measurements, cyclic voltammetry and differential-pulse voltammetry (CV and DPV, respectively), in the presence of two supporting electrolytes: $[^nBu_4N][PF_6]$ and $[^nBu_4N][BAr^F{}_4]$ (where Ar^F = $C_6H_3(CF_3)_2$-3,5) in dichloromethane. $[^nBu_4N][BAr^F{}_4]$ was better for this interaction than $[^nBu_4N][PF_6]$.

RESULTS AND DISCUSSION

Synthesis and Characterization of Heterobimetallic Pt_4Fe_n (n = 2, 3, and 4) Complexes. Treatment of **1** with excess amounts of **5** in a mixture of chloroform and methanol, followed by the removal of volatiles under reduced pressure and the

Received: May 13, 2011
Published: October 18, 2011

   dx.doi.org/10.1021/ic201012m | Inorg. Chem. 2011, 50, 11384–11393

Chart 1

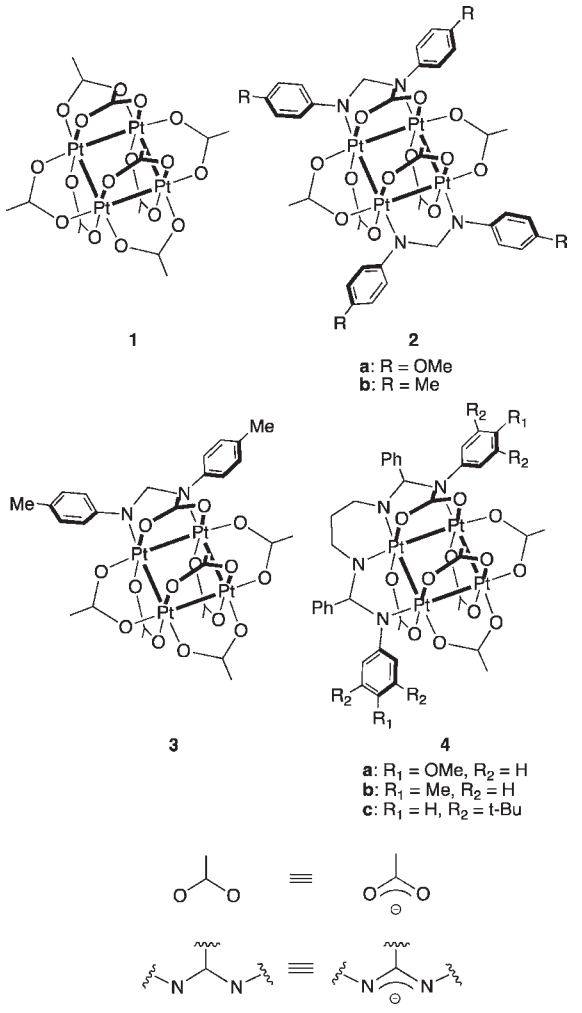

addition of solvents, and then repetition of these operations, afforded a tetrasubstituted complex $[Pt_4(\mu\text{-}OCOCH_3)_4(\mu\text{-}OCOC_5H_4FeCp)_4]$ (**6**) quantitatively (see eq 1).

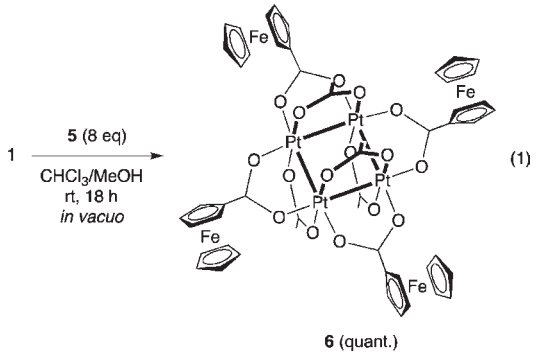

The same reaction under atmospheric pressure resulted in a complicated mixture of **6** and partially substituted complexes such as monosubstituted, disubstituted, and trisubstituted complexes, together with the starting complex **1**. Removal of the liberated acetic acid clearly shifted the equilibrium among all possible species bearing a labile *in-plane* acetate ligand to **6**. Similar methodology for the removal of liberated acetic acid

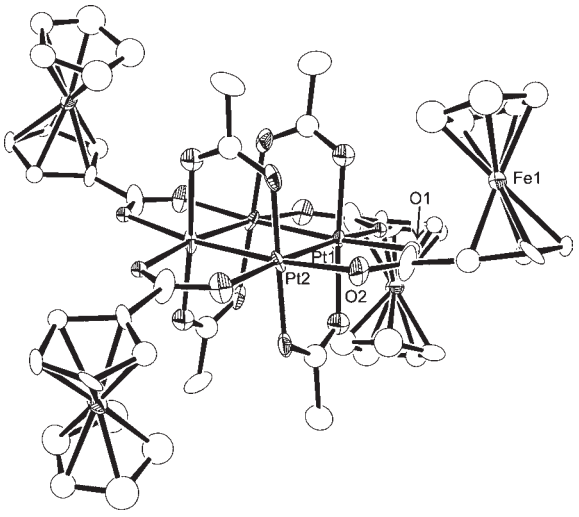

Figure 1. Molecular structure of **6** with thermal ellipsoids at 50% probability. All H atoms and the solvent molecule (toluene) were omitted for the sake of clarity.

Table 1. Selected Bond Distances and Separations between Two Fe Centers in Complexes 6, 8a, 8e, 8f, and 9b

	Bond Distance (Å)				
complex	Pt···Pt	mean Pt−^{ax}O	mean Pt−^{eq}O	mean Pt−N	Fe···Fe
6	2.5054(9)	2.03	2.13		11.914 (*trans*)
					10.030 (*cis*)
8a	2.5116(3), 2.5430(3)	2.02	2.16	2.16	13.200
	2.5154(3), 2.5402(3)				
8e	2.5299(4), 2.5309(4)	2.01	2.17	2.16	13.054
	2.4908(4), 2.5278(4)				
8f	2.5017(9), 2.5276(10)	2.02	2.21	2.19	11.710
	2.5080(9), 2.5250(10)				
9b					
Δ-isomer	2.5230(4), 2.5170(3)	2.02	2.23	2.11	10.428
Δ-isomer	2.5184(4), 2.5219(3)				
Λ-isomer	2.5336(3), 2.5360(4)	2.02	2.20	2.12	10.093
Λ-isomer	2.5264(3), 2.5195(4)				

was already reported for paddle-wheel Rh and Ru complexes.[14g] Complex **6** was characterized by spectral data and combustion analysis. The ^{1}H NMR spectrum of **6** showed a singlet at δ 2.03, which was due to four ^{ax}OAc ligands at the Pt_4 core, indicating that the four *in-plane* acetates were fully substituted. With regard to the ferrocene moiety, C_5H_4 ring protons were observed as two triplets at δ 4.45 and 5.21, while a singlet that was assigned to Cp ring protons appeared at δ 4.28.

Single crystals of **6** suitable for X-ray analysis were obtained in a toluene/hexane mixed solution, and its structure was determined crystallographically. The molecular structure of **6** is depicted in Figure 1, and its selected bond distances and the separation between Fe centers are summarized in Table 1. Notably, two FeCp moieties on the *trans* side of the Pt_4 unit were pointed in the same direction (*cis*), on the basis of the Pt_4

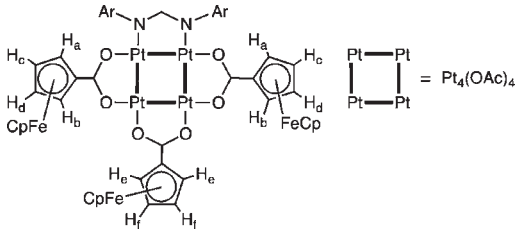

Figure 2. Numbering scheme of ring protons in three η^5-C_5H_4 moieties of complex **7**.

Scheme 1. Synthesis of 8a−8f

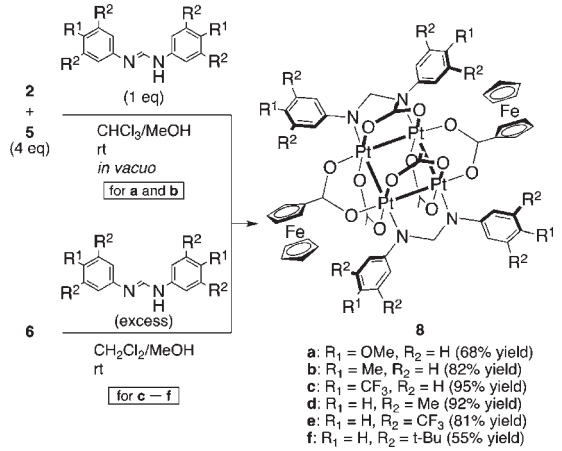

plane, whereas those on the *cis* side of the Pt_4 unit pointed in the opposite direction (*trans*). The mean bond distances of the Pt−^{eq}O bond (2.13 Å), the Pt−^{ax}O bond (2.03 Å), and the Pt···Pt distance (2.5054(9) Å) are comparable to those of the parent complex **1** (2.162 Å for the mean Pt−^{eq}O bond, 2.002 Å for the mean Pt−^{ax}O bond, and 2.495 Å for the mean Pt···Pt distance).[23] The distance between the two Fe atoms is 11.914 Å in the *trans* manner and 10.030 Å in the *cis* manner.

Three *in-plane* acetates of a *mono*-capped complex **3**, in which one side of the square Pt_4 core was occupied by an amidinate ligand, were replaced by **5** upon removal of the free acetic acid under the reduced pressure, leading to the isolation of $[Pt_4(\mu\text{-}OCOCH_3)_4(\mu\text{-}ArNCHNAr)(\mu\text{-}OCOC_5H_4FeCp)_3]$, where Ar = C_6H_4Me-4 (**7**) in 82% yield (eq 2).

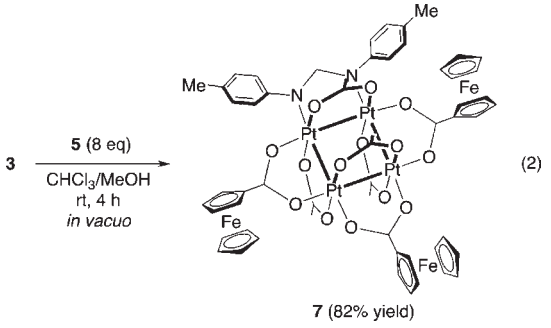

Complex **7** was characterized by nuclear magnetic resonance (NMR) and mass spectroscopy (MS), together with combustion analysis. The ^{1}H NMR spectrum of **7** showed three singlets at δ 1.96, 1.97, and 2.00 in a 1:2:1 integral ratio, which was due to the magnetically nonequivalent, four *out-plane* acetate protons, and

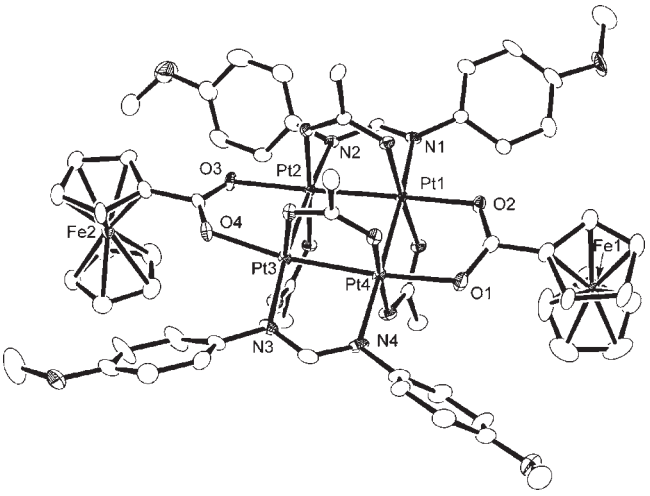

Figure 3. Molecular structure of **8a** with thermal ellipsoids at 50% probability. All H atoms and solvent molecules ($CHCl_3$) were omitted for the sake of clarity.

no signals due to the *in-plane* acetates, which was consistent with full replacement of the three *in-plane* acetates. For ferrocene moieties, two singlets at δ 4.17 and 4.25 in a 2:1 relative ratio were assigned to two nonequivalent Cps (*cis* and *trans* to the amidinate ligand). Because of the unsymmetrical environment of the ferrocenyl moieties at the *cis* position to the amidinate ligand, the four protons (H_a, H_b, H_c, and H_d) of two C_5H_4COO moieties *cis* to the amidinate ligand were magnetically nonequivalent. In addition, one C_5H_4COO moiety *trans* to the amidinate ligand had two types of protons (H_e and H_f). Accordingly, a total of six magnetically nonequivalent protons were observed as a multiplet around δ 4.35−4.38 for H_c, H_d, and H_f: two broad signals at δ 4.86 and 5.02 for H_a and H_b: and a triplet at δ 5.18 for H_e in a 3:1:1:1 integral ratio (see Figure 2).

We conducted the reaction of a *trans*-capped Pt_4 complex *trans*-$[Pt_4(\mu\text{-}OCOCH_3)_6(\mu\text{-}ArNCHNAr)_2]$, where Ar = C_6H_4Me-4) (**2b**) with excess amounts of **5** in a mixture of chloroform and methanol to give a mixture of the trisubstituted complex **7** and a *trans*-disubstituted Pt_4 complex, *trans*-$[Pt_4(\mu\text{-}OCOCH_3)_4(\mu\text{-}ArNCHNAr)_2(\mu\text{-}OCOC_5H_4FeCp)_2]$ (**8b** = Ar = C_6H_4Me-4). Examination of the reaction conditions to isolate the *trans*-disubstituted Pt_4 complex **8b** revealed that the treatment of **2b** with 4 equiv of **5** in the presence of 1 equiv of the corresponding amidine ligand under reduced pressure was optimal, affording **8b** in 82% yield (Scheme 1). Such a successful isolation of **8b** was attributed to the addition of 1 equiv of the amidine ligand, which prevented the contamination of **7**. Similarly, $[Pt_4(\mu\text{-}OCOCH_3)_4(\mu\text{-}ArNCHNAr)_2(\mu\text{-}OCOC_5H_4FeCp)_2]$, where Ar = C_6H_4OMe-4) was obtained in 68% yield from **2a** and **5** (Scheme 1) (**8a**). Another synthetic route was the reaction of the tetrasubstituted Pt_4 complex **6** with excess amounts of an amidine ligand (Scheme 1). In this protocol, *trans*-disubstituted Pt_4 complexes **8c**−**8f** were isolated in moderate to good yield upon treating **6** with the corresponding amidine ligand. The ^{1}H NMR spectra of complexes **8a**−**8f** displayed two singlet signals assignable to ^{ax}OAc parallel to the side divided by two amidinate ligands in the *trans* positions of the Pt_4 square and ^{ax}OAc perpendicular to the side, along with one set of signals due to Cp and C_5H_4 ring protons of the two ferrocene moieties. The $^{13}C\{^1H\}$ NMR spectra of **8a**−**8f** displayed two of the same *trans*-arranged two ferrocene pendants.

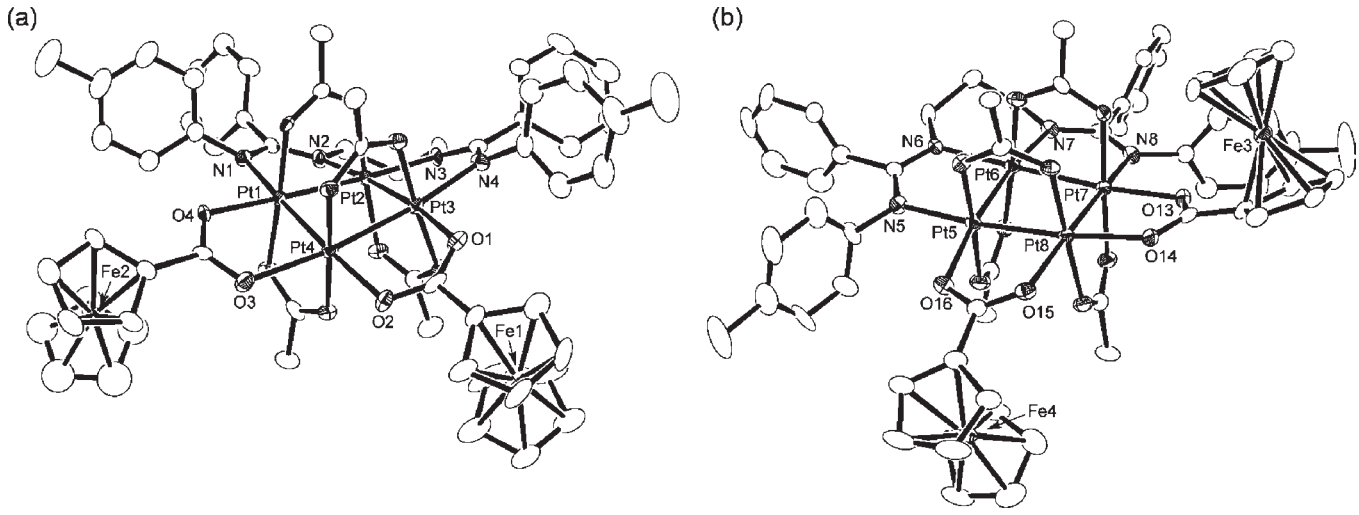

Figure 4. Molecular structures of (a) the Δ-isomer and (b) the Λ-isomer of **9b** with thermal ellipsoids at 50% probability. All H atoms and the solvent molecule ($CHCl_3$) were omitted for the sake of clarity.

The solid-state structures of **8a**, **8e**, and **8f** were crystallographically determined, and their selected bond distances and the separation between the two iron centers are summarized in Table 1. Figure 3 shows the structure of **8a**, while structures of **8e** and **8f** are depicted in the Supporting Information (Figures S1 and S2), because they had the same geometry around the Pt_4 moiety as **8a**. Two ferrocenecarboxylate ligands occupied the *trans* sides of the Pt_4 unit, and the best planes of two C_5H_4 ring carbons are coplanar with that of the Pt_4 unit, evidenced by the small dihedral angles between the respective planes, 9.06° and 12.83°. Interestingly, **8a** and **8f** adopted the *cis*-orientation mode of the two FeCp moieties referring to the Pt_4 plane, while **8e** adopted a *trans*-direction mode. Bond distances and angles within the Pt_4 unit are normal and comparable to those of **2a**:[2Sb] the mean Pt−^{eq}O bond (2.16 Å), Pt−N bond (2.16 Å), and Pt···Pt distances of **8a** (2.528 Å) are comparable to those of **2a** (2.17 Å for the mean Pt−^{eq}O bond, 2.14 Å for the mean Pt−N bond, 2.529 Å for the mean Pt···Pt distance). The distance between the two Fe atoms of **8a** is 13.200 Å.

Reaction of the *cis*-capped complexes **4a**−**4c** with 2 equiv of **5** proceeded under reduced pressure to give the corresponding *cis*-disubstituted complexes $[Pt_4(\mu\text{-}OCOCH_3)_4(\kappa^4\text{-}N_4\text{-}DArBp)(\mu\text{-}OCOC_5H_4FeCp)_2]$, where DArBp = *N*,*N*′-bis((4-anisyl)benzamidinato)propane (**9a**), *N*,*N*′-bis((4-tolyl)benzamidinato)propane (**9b**), or *N*,*N*′-bis((3,5-di-*tert*-butylphenyl)benzamidinato)propane (**9c**) (see eq 3).

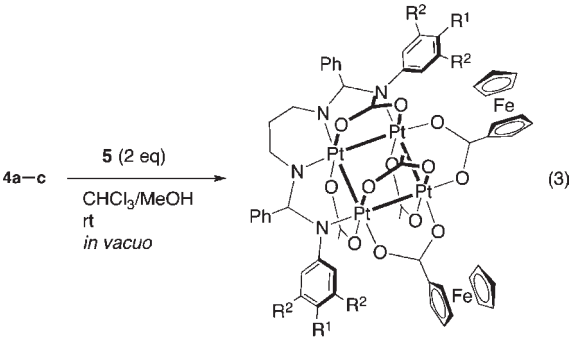

(3)

The structures of complexes **9a**−**9c** were confirmed by NMR spectroscopy, electrospray ionization−mass spectroscopy (ESI-MS), combustion analysis, and single-crystal X-ray analysis for **9b**. In the ^{1}H NMR spectrum of **9a**−**9c**, two singlets were assigned to two magnetically nonequivalent ^{ax}OAc species. For the ferrocene units, the Cp ring protons were observed as a singlet, and the four ring protons of the C_5H_4 moiety in **9a** and **9b** were observed as a triplet and two multiplets in a 2:1:1 integral ratio, whereas those of **9c** were observed as four broad signals in a 1:1:1:1 integral ratio. The $^{13}C\{^1H\}$ NMR spectra of **9a**−**9c** displayed two of the same *cis*-arranged ferrocene pendants.

Figure 4 shows the molecular structures of the Δ- and Λ-isomers of **9b**, which are independent molecules in the unit cell. The selected bond distances and the separation between the two Fe centers are listed in Table 1. A notable structural feature is that the FeCp moieties in the Δ- and Λ-isomers have different orientations: the two FeCp moieties in the Δ-isomer are pointed in the same direction (*cis*), while those of the Λ-isomer are pointed in the opposite direction (*trans*). Bond distances and angles within the Pt_4 unit are normal and comparable to those of the *cis*-capped Pt_4 complexes. The distance between the two Fe atoms are 10.428 Å for the Δ-isomer and 10.093 Å for the Λ-isomer; these values are clearly shorter than those of the complexes of **8**.

Electrochemical Properties of Pt_4−Fe_n (n = 2, 3, and 4) Complexes 6−9. The redox behavior of heterometallic complexes **6**−**9**, which are comprised of a Pt_4 core and two or more ferrocene units was investigated using CV and DPV recorded in dichloromethane solution containing 0.1 M $[^nBu_4N][PF_6]$ or $[^nBu_4N][BAr^F{}_4]$ (Ar^F = $C_6H_3(CF_3)_2$-3,5) as the supporting electrolyte. First, we measured the CV and DPV of *trans*-Pt_4Fe_2 complexes **8a**−**8f** with $[^nBu_4N][PF_6]$ and determined the $E_{1/2}$ values of each oxidation event. The $\Delta E_{1/2}$ and K_c values[27] corresponding to the oxidation of ferrocene moieties are listed in Table 2. The CV and DPV of **8a** gave three oxidation processes, which are referenced as **A**, **B**, and **C** (see Figures 5a and 6a). Based on the reported oxidation potential of ferrocene derivatives and the parent complex **2a**,[2Sb] wave **A** was determined to be a reversible oxidation event that was due to the two ferrocene pendants (Fe^{3+}/Fe^{2+}), and waves **B** and **C** were assigned to one electron oxidation process each of $Pt_4{}^{9+}/Pt_4{}^{8+}$ and $Pt_4{}^{10+}/Pt_4{}^{9+}$, respectively. The CV and DPV of **8b** and **8f**

dx.doi.org/10.1021/ic201012m |*Inorg. Chem.* 2011, 50, 11384–11393

Table 2. $E_{1/2}$ (mV vs Fc^+/Fc), $\Delta E_{1/2}$, and K_c of 8a−8f and 9a−9c Determined by DPV Analysis in a 1 mM Dichloromethane Solution Containing 0.1 M $[^nBu_4N][PF_6]$ and $[^nBu_4N][BAr^F{}_4]$

	$E_{1/2}$ (mV vs Fc^+/Fc)				
electrolyte	**A** (Fe^{3+}/Fe^{2+})	**B** (Pt_4^{9+}/Pt_4^{8+})	**C** (Pt_4^{10+}/Pt_4^{9+})	$\Delta E_{1/2}$ (mV)[a]	K_c[b]
complex **8a**					
$[^nBu_4N][PF_6]$	180	410	670		
$[^nBu_4N][BAr^F{}_4]$	140, 200	470	860	70	20
complex **8b**					
$[^nBu_4N][PF_6]$	150	560	860		
$[^nBu_4N][BAr^F{}_4]$	140, 200	640		60	10
complex **8c**					
$[^nBu_4N][PF_6]$	220	990			
$[^nBu_4N][BAr^F{}_4]$	190, 260			70	20
complex **8d**					
$[^nBu_4N][PF_6]$	180	560			
$[^nBu_4N][BAr^F{}_4]$	120, 200	680		80	20
complex **8e**					
$[^nBu_4N][PF_6]$	230				
$[^nBu_4N][BAr^F{}_4]$	190, 280			100	42
complex **8f**					
$[^nBu_4N][PF_6]$	140, 210	640	940	70	20
$[^nBu_4N][BAr^F{}_4]$	120, 230	700		110	78
complex **9a**					
$[^nBu_4N][PF_6]$	100	540	720		
$[^nBu_4N][BAr^F{}_4]$	40, 100	610		60	10
complex **9b**					
$[^nBu_4N][PF_6]$	90	680	900		
$[^nBu_4N][BAr^F{}_4]$	30, 100			80	20
complex **9c**					
$[^nBu_4N][PF_6]$	90	670[c]			
$[^nBu_4N][BAr^F{}_4]$	10, 100			90	40

[a] This value was determined as difference between two peaks in process **A**. [b] This value was defined as $Fc-[Pt_4]-Fc + Fc^+-[Pt_4]-Fc^+ \overset{K_c}{\rightleftharpoons} Fc-[Pt_4]-Fc^+$, where Fc is defined as the $FeCp(C_5H_4COO)$ moiety and $K_c = \exp(\Delta E_{1/2}/25.69)$. [c] This value was determined by cyclic voltammetry (CV), because no wave corresponding to process **B** was observed in differential-pulse voltammetry (DPV).

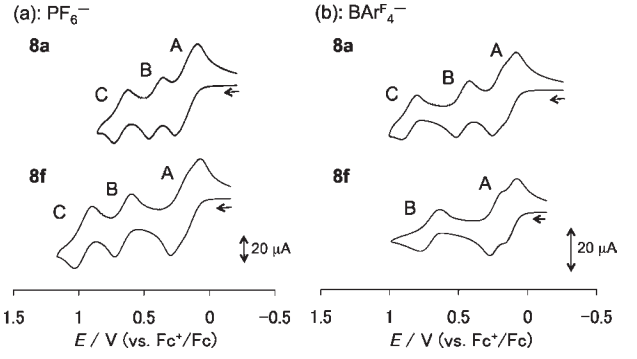

Figure 5. Cyclic voltammetry (CV) voltammograms of **8a** (top) and **8f** (bottom) recorded in 1 mM dichloromethane solution containing (a) 0.1 M $[^nBu_4N][PF_6]$ and (b) 0.1 M $[^nBu_4N][BAr^F{}_4]$, using a scan rate of 100 mV/s.

(Figure 5a) also exhibited three oxidation processes, also labeled as **A**, **B**, and **C**. In contrast, complexes **8c** and **8d** showed two oxidation processes **A** and **B**, and complex **8e** exhibited only one oxidation process (**A**) (see Table 2). Remarkably, process **A** of complex **8f** was separated into two peaks with a $\Delta E_{1/2}$ value of 70 mV, indicating an interaction between the two ferrocene moieties of **8f** (see Table 2 and Figure 6a).

By changing the supporting electrolyte from $[^nBu_4N][PF_6]$ to $[^nBu_4N][BAr^F{}_4]$, the CV and DPV of **8a**−**8f** were measured. The electrochemical data and DPV of the peaks due to the oxidation of ferrocene moieties (process **A**) are summarized in Table 2 and Figure 6b, respectively. Notably, the oxidation events at the two ferrocene moieties (**A**) of **8a**−**8f** were observed as separated peaks, in sharp contrast to the unresolved peak in $[^nBu_4N][PF_6]$ solution, except for complex **8f**, and their $\Delta E_{1/2}$ values [70 mV (**8a**), 60 mV (**8b**), 70 mV (**8c**), 80 mV (**8d**), 100 mV (**8e**), and 110 mV (**8f**)] tended to increase as the bulkiness of the amidinate ligands increased. These observations strongly suggested that two ferrocene moieties in complexes **8a**−**8f** with $[^nBu_4N][BAr^F{}_4]$ interact with each other through the $[Pt_4(OAc)_4]^{4+}$ spacer more effectively than that with $[^nBu_4N][PF_6]$, despite the long distance (11.7—13.2 Å) between the Fe centers.[28−30]

The CV and DPV of **9a**−**9c** were also measured in dichloromethane containing two types of electrolytes (see Figures 7 and 8, as well as Table 2). The CV of complexes **9a** and **9b** with $[^nBu_4N][PF_6]$ had three oxidation processes (**A** (Fe^{3+}/Fe^{2+}), **B** (Pt_4^{9+}/Pt_4^{8+}), and **C** (Pt_4^{10+}/Pt_4^{9+})), while that of complex **9c**

dx.doi.org/10.1021/ic201012m |Inorg. Chem. 2011, 50, 11384–11393

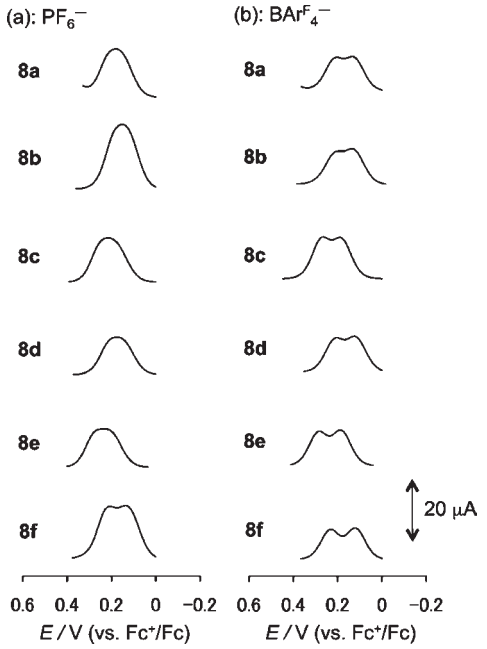

Figure 6. Peaks due to ferrocene moieties of **8a**−**8f** (from top to bottom) in differential-pulse voltammetry (DPV) recorded in a 1 mM dichloromethane solution containing (a) 0.1 M [^{n}Bu$_4$N][PF$_6$] and (b) 0.1 M [^{n}Bu$_4$N][BAr$^F_4$].

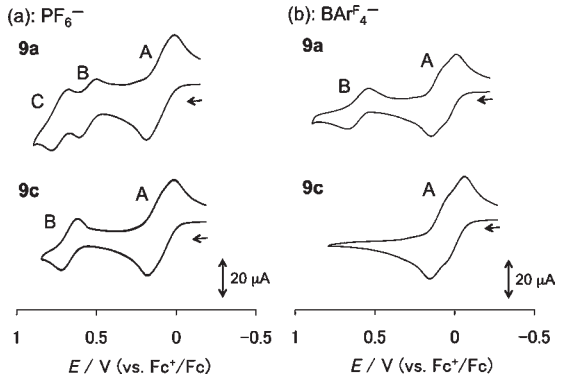

Figure 7. CV voltammograms of **9a** (top) and **9c** (bottom) recorded in a 1 mM dichloromethane solution containing (a) 0.1 M [^{n}Bu$_4$N][PF$_6$] and (b) 0.1 M [^{n}Bu$_4$N][BAr$^F_4$], using a scan rate of 100 mV/s.

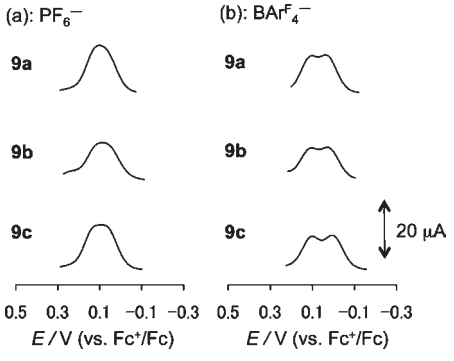

Figure 8. Peaks due to ferrocene moieties of **9a**−**9c** in DPV recorded in 1 mM dichloromethane solution containing (a) 0.1 M [^{n}Bu$_4$N][PF$_6$] and (b) 0.1 M [^{n}Bu$_4$N][BAr$^F_4$].

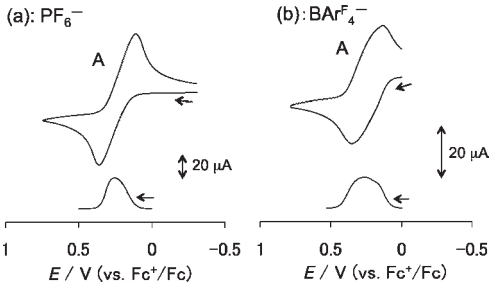

Figure 9. CV and DPV voltammograms of **6** recorded in (a) 1 mM dichloromethane solution containing 0.1 M [^{n}Bu$_4$N][PF$_6$], using a scan rate of 100 mV/s, and (b) 0.5 mM dichloromethane solution containing 0.1 M [^{n}Bu$_4$N][BAr$^F_4$], using a scan rate of 100 mV/s.

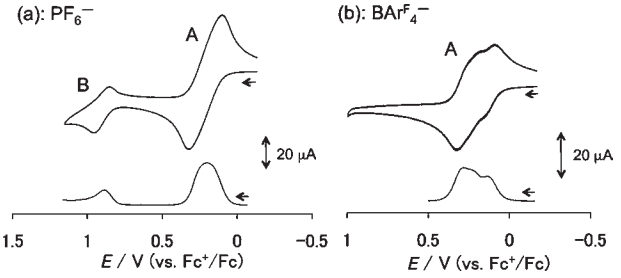

Figure 10. CV and DPV voltammograms of **7** recorded in 1 mM dichloromethane solution containing (a) 0.1 M [^{n}Bu$_4$N][PF$_6$] and (b) 0.1 M [^{n}Bu$_4$N][BAr$^F_4$], using a scan rate of 100 mV/s.

with [^{n}Bu$_4$N][PF$_6$] had two oxidation processes (**A** and **B**). In voltammetry measurements with [^{n}Bu$_4$N][BAr$^F_4$], complex **9a** had waves **A** and **B**; however, complexes **9b** and **9c** afforded only wave **A**. Although process **A** in DPV with [^{n}Bu$_4$N][PF$_6$] was observed as an unresolved peak, process **A** in DPV with [^{n}Bu$_4$N][BAr$^F_4$] was split into two peaks (see Figure 8), suggesting an weak interaction between the two ferrocene units in *cis*-Pt$_4$Fe$_2$ complexes **9a**−**9c** with [^{n}Bu$_4$N][BAr$^F_4$]. The $\Delta E_{1/2}$ and K_c values of **9c** (90 mV and 40, respectively) were larger than those of **9a** and **9b** (60 mV, 10 for **9a**; 80 mV, 20 for **9b**).

Geiger and his co-workers previously reported this type of counteranion effect, which was due to the combination of solvent and electrolyte anions affecting the oxidation events of neutral complexes.[31,32] In particular, supporting electrolytes containing weakly coordinating anions such as B(C$_6$F$_5$)$_4^-$ or BAr$^F_4{}^-$ in nonpolar solvents increased the $\Delta E_{1/2}$ value of multiferrocene complexes, because of a minimized ion-pairing effect, resulting in an electrostatic interaction between redox active ferrocene centers. Our observation that the $\Delta E_{1/2}$ value was increased with a much bulkier aryl group at the amidinate ligands suggested an electrostatic interaction that was probably due to a shielding effect,[29] although we could not rule out the contribution of electronic interaction that was due to the similarity in the magnitude of the interaction between the *cis*- and *trans*-arranged complexes, in which the distance between the two ferrocene units was different.[30]

The CV and DPV voltammograms of **6** with [^{n}Bu$_4$N][PF$_6$] and [^{n}Bu$_4$N][BAr$^F_4$] are shown in Figure 9, in which one reversible oxidation process (labeled as **A**) was attributed to four-electron oxidation of ferrocenyl moieties (Fe^{3+}/Fe^{2+}). For complex **6**, no obvious difference due to the supporting electrolyte was observed, although peak **A** in DPV in [^{n}Bu$_4$N][BAr$^F_4$] was broader than that in [^{n}Bu$_4$N][PF$_6$].[29]

We electrochemically studied the Pt_4Fe_3 complex **7**, in which two ferrocene units were present at the *cis* position to the amidinate ligand and one ferrocene unit was present *trans* to the amidinate ligand (see Figure 10). The CV and DPV of **7** in both electrolytes displayed two oxidation waves, referenced as **A** (Fe^{3+}/Fe^{2+}) and **B** (Pt_4^{9+}/Pt_4^{8+}). In the DPV in [^{n}Bu$_4$N][BAr$^F_4$], oxidation event **A**, which was due to the oxidation process of the ferrocene units, was split into two dissymmetric peaks, presumably because of the separation of two types of nonequivalent ferrocene units at positions *cis* and *trans* to the amidinate ligand (see Figure 10b).

CONCLUSION

In summary, we synthesized four types of Pt_4 complexes **6**−**9** with ferrocene pendants and revealed their redox properties using electrochemical measurements with [^{n}Bu$_4$N][PF$_6$] and [^{n}Bu$_4$N][BAr$^F_4$] as supporting electrolytes. Using cyclic voltammetry (CV) and differential-pulse voltammetry (DPV), oxidation events due to process **A** (Fe^{3+}/Fe^{2+}) for *trans*-Pt_4Fe_2 complexes **8a**−**8f** with [^{n}Bu$_4$N][BAr$^F_4$] and *cis*-Pt_4Fe_2 complexes **9a**−**9c** with [^{n}Bu$_4$N][BAr$^F_4$] exhibited two separate peaks, indicating weak interaction between the two ferrocene units, despite the geometrical difference between **8** (*cis*) and **9** (*trans*), with respect to the Pt_4 core. In DPV of both complexes **8** and **9**, the magnitudes of the $\Delta E_{1/2}$ and K_c values were dependent on the steric bulkiness of the aryl moieties of the amidinate ligand, and were independent of the electronic properties of the aryl ligand, characterizing the interaction between ferrocene units as an electrostatic interaction derived from a shielding effect with some orbital interaction contribution.

EXPERIMENTAL SECTION

General Procedures. All manipulations were conducted utilizing standard Schlenk tubes and high-vacuum line techniques under an atmosphere of argon. Solvents were distilled under an atmosphere of argon from sodium benzophenone ketyl (Et_2O), P_2O_5 (CH_2Cl_2), and $Mg(OMe)_2$ (methanol, MeOH). Dehydrated CD_2Cl_2 and $CDCl_3$ were degassed and stored under an atmosphere of argon over activated MS (4 Å). Other reagents, including [FeCp(η^5-C_5H_4COOH)] (**5**), purchased from commercial sources, were used without further purification. [$Pt_4(\mu$-OCOCH$_3)_8$] (**1**),[24a] [$Pt_4(\mu$-OCOCH$_3)_6(\mu$-ArNCHNAr$)_2$] (where Ar = C_6H_4OMe-4 (**2a**) or C_6H_4Me-4 (**2b**)),[25b] [$Pt_4(\mu$-OCOCH$_3)_7(\mu$-ArNCHNAr)] (Ar = C_6H_4Me-4; **3**),[25b] and *cis*-[$Pt_4(\mu$-OCOCH$_3)_6(\kappa^4$-*N*$_4$-DArBp)] (where DArBp = 1,3-bis(*N*,*N*′-di(*p*-anisyl)benzamidinate)propane (**4a**), 1,3-bis(*N*,*N*′-di(*p*-tolyl)benzamidinate)propane (**4b**), or 1,3-bis(*N*,*N*′-di(C_6H_3(^{t}Bu)$_2$-3,5)benzamidinate)propane) (**4c**)),[25a] and *N*,*N*′-bis(aryl)formamidine (where aryl = $C_6H_4CF_3$-4, $C_6H_4Me_2$-3,5, $C_6H_4(CF_3)_2$-3,5, and C_6H_4(^{t}Bu)$_2$-3,5)[33] were prepared according to the literature, although **4c** was a new compound. A Mercury-300 Fourier transform spectrometer (Varian) or BRUKER AVANCEIII-400 spectrometer (Bruker Avance) was used for NMR spectroscopy, and all spectra were recorded at a temperature of 30 or 35 °C, unless mentioned otherwise: ^{1}H and ^{13}C NMR spectra were referenced to an internal solvent and corrected to tetramethylsilane, $SiMe_4$, and ^{19}F{^{1}H} NMR spectra were referenced to an external reference of trifluorotoluene at (δ = 63.9 ppm). Mass spectrometric data were obtained using ESI or FAB techniques (on a JEOL Model SX-102 spectrometer) or ESI techniques (on a Bruker micrOTOF spectrometer). Elemental analyses were recorded on a Perkin−Elmer Model 2400II microanalyzer at the Department of Chemistry, Faculty of Engineering Science, Osaka University. Melting points were measured in sealed tubes and were not corrected.

Preparation of [$Pt_4(\mu$-OCOCH$_3)_4(\mu$-OCOC$_5$H$_4$FeCp$)_4$] (6). To a solution of **1** (410 mg, 0.327 mmol) in $CHCl_3$ (8 mL) was added a solution of ferrocenecarboxylic acid (**5**) (635 mg, 2.76 mmol, 8 equiv) in a mixture of $CHCl_3$ (7 mL) and methanol (15 mL). The reaction mixture was stirred for 12 h at ambient temperature under reduced pressure. During this operation, a mixture of $CHCl_3$ (10 mL) and methanol (10 mL) were repeatedly added before all volatiles were completely removed. Removal of all of the volatiles gave a solid, which was washed with methanol (20 mL, four times), leaving complex **6** as a brown powder (731 mg, quant.), mp 209−212 °C (decomp.). ^{1}H NMR (300 MHz, $CDCl_3$, 35 °C, δ/ppm): 2.03 (s, 12H, $^{ax}CH_3CO_2$), 4.28 (s, 20H, Cp H), 4.45 (t, $^3J_{HH}$ = 2 Hz, 8H, −C_5H_4), 5.21 (t, $^3J_{HH}$ = 2 Hz, 8H, −C_5H_4); MS (ESI positive, CH_3CN): *m*/*z*: 1932 [*M*]$^+$. Anal. Calcd for $C_{52}H_{48}Fe_4O_{16}Pt_4$: C 32.32, H 2.52. Found: C 32.67, H 2.28. The ^{13}C{^{1}H} NMR spectrum was not measured, because of the low solubility of **6**.

Preparation of [$Pt_4(\mu$-OCOCH$_3)_4(\mu$-OCOC$_5$H$_4$FeCp$)_3(\mu$-ArNCHNAr)] (7: Ar = C_6H_4Me-4). To a mixture of **3** (49.9 mg, 0.0352 mmol) and **5** (64.8 mg, 0.282 mmol, 8 equiv) was added a mixture of $CHCl_3$ (3 mL) and methanol (3 mL). The reaction mixture was stirred for 4 h at ambient temperature under the same reduced pressure. After removal of all of the volatiles, the resulting solid was washed with methanol (5 mL, twice) to give **7** as a reddish brown powder (55.6 mg, 82% yield), mp 206−210 °C (decomp.). ^{1}H NMR (400 MHz, $CDCl_3$, 30 °C, δ/ppm): 1.96 (s, 3H, $^{ax}CH_3CO_2$), 1.97 (s, 6H, $^{ax}CH_3CO_2$), 2.00 (s, 3H, $^{ax}CH_3CO_2$), 2.46 (s, 6H, −$C_6H_4CH_3$), 4.17 (s, 10H, Cp H), 4.25 (s, 5H, Cp H), 4.35−4.38 (m, 6H, −C_5H_4), 4.86 (br q, 2H, −C_5H_4), 5.02 (br q, 2H, −C_5H_4), 5.18 (t, $^3J_{HH}$ = 2 Hz, 2H, −C_5H_4), 6.63 (s, 1H, −NCHN−), 7.30 (d, $^3J_{HH}$ = 8.0 Hz, 4H, −$C_6H_4CH_3$), 7.39 (d, $^3J_{HH}$ = 8.0 Hz, 4H, −$C_6H_4CH_3$). MS (ESI positive, CH_3CN): *m*/*z*: 1949 [*M*+Na]$^+$. Anal. Calcd for $C_{56}H_{54}Fe_3N_2O_{14}Pt_4$: C 34.91, H 2.82, N 1.45. Found: C 34.90, H 2.43, N 1.40. The ^{13}C{^{1}H} NMR spectrum was not measured, because of the low solubility of **7**.

Preparation of [$Pt_4(\mu$-OCOCH$_3)_4(\mu$-OCOC$_5$H$_4$FeCp$)_2(\mu$-ArNCHNAr$)_2$]. *8a*: *Ar* = C_6H_4OMe-4. A reaction mixture of **2a** (162 mg, 0.0985 mmol), **5** (90.8 mg, 0.375 mmol, 3.8 equiv), and *N*,*N*′-di(*p*-anisyl)formamidine (24.1 mg, 0.0940 mmol, 1.0 equiv.) in the mixture of $CHCl_3$ (5 mL) and MeOH (5 mL) was stirred for 12 h at ambient temperature under reduced pressure. After the resulting solid was washed with MeOH (5 mL, twice), complex 8a was obtained as reddish brown powders (133 mg, 68% yield), mp 225−228 °C (decomp.). ^{1}H NMR (400 MHz, $CDCl_3$, 30 °C, δ/ppm): 1.88 (s, 6H, $^{ax}CH_3CO_2$), 1.95 (s, 6H, $^{ax}CH_3CO_2$), 3.89 (s, 12H, −$C_6H_4OCH_3$), 4.09 (s, 10H, Cp H), 4.28 (t, $^3J_{HH}$ = 2 Hz, 4H, −C_5H_4), 4.73 (t, $^3J_{HH}$ = 2 Hz, 4H, −C_5H_4), 6.94 (s, 2H, −NCHN−), 7.00 (d, $^3J_{HH}$ = 8.8 Hz, 8H, −$C_6H_4OCH_3$), 7.38 (d, $^3J_{HH}$ = 8.8 Hz, 8H, −$C_6H_4OCH_3$). ^{13}C{^{1}H} NMR (100 MHz, $CDCl_3$, 30 °C, δ/ppm): 21.4, 22.0 (s, $^{ax}CH_3CO_2$), 55.7 (s, −$C_6H_4OCH_3$), 69.8 (s, Cp C), 70.7, 70.8, 73.2 (s, −C_5H_4), 113.7, 125.6, 143.2, 156.2 (s, Ar C), 161.5 (s, −NCHN−), 185.1 (s, −$OCOC_5H_4$), 191.4, 193.9 (s, $^{ax}CH_3CO_2$). MS (ESI positive, CH_3CN): *m*/*z*: 1729 [*M*—ArNCHNAr]$^+$, 1985 [*M*+H]$^+$. Anal. Calcd for $C_{60}H_{60}Fe_2N_4O_{16}Pt_4$: C 36.30, H 3.05, N 2.82. Found: C 36.15, H 2.72, N 2.84.

Similar operations were conducted for the preparation of [$Pt_4(\mu$-OCOCH$_3)_4(\mu$-OCOC$_5$H$_4$FeCp$)_2(\mu$-ArNCHNAr$)_2$] where Ar = C_6H_4Me-4 (**8b**).

8b: *Ar* = C_6H_4*Me-4.* **8b** was generated in the form of a dark red powder (82% yield), mp 218−221 °C (decomp.) ^{1}H NMR (300 MHz, $CDCl_3$, 35 °C, δ/ppm): 1.86 (s, 6H, $^{ax}CH_3CO_2$), 1.93 (s, 6H, $^{ax}CH_3CO_2$), 2.43 (s, 12H, −$C_6H_4CH_3$), 4.11 (s, 10H, Cp H), 4.30 (t, $^3J_{HH}$ = 2 Hz, 4H, −C_5H_4), 4.74 (t, $^3J_{HH}$ = 2 Hz, 4H, −C_5H_4), 6.99 (s, 2H, −NCHN−), 7.24 (d, $^3J_{HH}$ = 8.3 Hz, 8H, −$C_6H_4CH_3$), 7.37 (d, $^3J_{HH}$ = 8.3 Hz, 8H,

$-C_6H_4CH_3$). $^{13}C\{^1H\}$ NMR (75 MHz, $CDCl_3$, 35 °C, δ/ppm): 21.0 (s, $-C_6H_4CH_3$), 21.4, 21.9 (s, $^{ax}CH_3CO_2$), 69.8 (s, Cp C), 70.6, 70.8, 73.2 (s, $-C_5H_4$), 124.6, 129.0, 132.8, 147.2 (s, Ar C), 161.9 (s, −NCHN−), 185.1 (s, $-OCOC_5H_4$), 191.5, 193.9 (s, $^{ax}CH_3CO_2$). MS (ESI positive, CH_3CN): *m/z*: 1920 $[M]^+$. Anal. Calcd for $C_{60}H_{60}Fe_2N_4O_{12}Pt_4 \cdot CH_2Cl_2$: C 36.52, H 3.12, N 2.79. Found: C 36.54, H 2.84, N 2.81.

8c: *Ar* = $C_6H_4CF_3$-*4*. A mixture of **6** (100 mg, 0.0517 mmol) and *N*,*N*′-di(*p*-trifluoromethylphenyl)formamidine (271 mg, 0.816 mmol, 16 equiv) in a mixed solvent of CH_2Cl_2 (30 mL) and methanol (20 mL) was stirred for 20 h at ambient temperature and for 22 h at 40 °C, and then all of the volatiles were removed under reduced pressure, followed by washing with methanol (5 mL, twice) to give **8c** as a reddish brown powder (105.3 mg, 95% yield), mp 236−238 (decomp.). ^1H NMR (400 MHz, $CDCl_3$, 30 °C, δ/ppm): 1.93 (s, 6H, $^{ax}CH_3CO_2$), 1.96 (s, 6H, $^{ax}CH_3CO_2$), 4.03 (s, 10H, Cp H), 4.34 (t, $^3J_{HH}$ = 2 Hz, 4H, $-C_5H_4$), 4.62 (t, $^3J_{HH}$ = 2 Hz, 4H, $-C_5H_4$), 7.10 (s, 2H, −NCHN−), 7.55 (d, $^3J_{HH}$ = 8.4 Hz, 8H, $-C_6H_4CF_3$), 7.72 (d, $^3J_{HH}$ = 8.4 Hz, 8H, $-C_6H_4CF_3$). $^{13}C\{^1H\}$ NMR (100 MHz, $CDCl_3$, 30 °C, δ/ppm): 21.5, 21.9 (s, $^{ax}CH_3CO_2$), 69.9 (s, Cp C), 70.7, 71.2, 72.3 (s, $-C_5H_4$), 123.7 (s, Ar C), 125.7 (q, $^3J_{CF}$ = 3.8 Hz, Ar C), 152.1 (s, Ar C), 152.4 (s, −NCHN−), 185.8 (s, $-OCOC_5H_4$), 192.1, 194.2 (s, $^{ax}CH_3CO_2$). One of the aromatic carbons and a $-CF_3$ group, which were flanked by a large coupling constant with fluorine, could not be identified, because of the low solubility of **8c**. ^{19}F NMR (376 MHz, $CDCl_3$, 30 °C, δ/ppm): −62.8 ($-C_6H_4CF_3$). MS (ESI positive, CH_3CN): *m/z*: 2136 $[M]^+$. Anal. Calcd for $C_{60}H_{48}F_{12}Fe_2N_4O_{12}Pt_4 \cdot CH_2Cl_2$: C 32.97, H 2.27, N 2.52. Found: C 32.74, H 2.47, N 2.17.

Similar procedures were conducted for the preparation of $[Pt_4(\mu\text{-}OCOCH_3)_4(\mu\text{-}OCOC_5H_4FeCp)_2(\mu\text{-}ArNCHNAr)_2]$ where Ar = $C_6H_3Me_2$-3,5 (**8d**), $C_6H_3(CF_3)_2$-3,5) (**8e**), and $[C_6H_3(^tBu)_2$-3,5) (**8f**).

8d: *Ar* = $C_6H_3Me_2$-*3,5*. **8d** was generated in the form of a brown powder (92% yield), mp 246−249 (decomp.). ^1H NMR (400 MHz, $CDCl_3$, 30 °C, δ/ppm): 1.91 (s, 6H, $^{ax}CH_3CO_2$), 1.98 (s, 6H, $^{ax}CH_3CO_2$), 2.44 (s, 24H, $-C_6H_3(CH_3)_2$), 4.09 (s, 10H, Cp H), 4.26 (t, $^3J_{HH}$ = 2 Hz, 4H, $-C_5H_4$), 4.71 (t, $^3J_{HH}$ = 2 Hz, 4H, $-C_5H_4$), 6.87 (br s, 4H, $-C_6H_3(CH_3)_2$), 6.97 (s, 2H, −NCHN−), 7.08 (br s, 8H, $-C_6H_3(CH_3)_2$). $^{13}C\{^1H\}$ NMR (100 MHz, $CDCl_3$, 30 °C, δ/ppm): 21.5, 22.0 (s, $^{ax}CH_3CO_2$), 21.6 (s, $-C_6H_3(CH_3)_2$), 69.9 (s, Cp C), 70.5, 71.0, 73.2 (s, $-C_5H_4$), 122.7, 125.4, 137.7, 149.6 (s, Ar C), 162.3 (s, −NCHN−), 185.2 (s, $-OCOC_5H_4$), 191.5, 193.8 (s, $^{ax}CH_3CO_2$). MS (ESI positive, CH_3CN): *m/z*: 1977 $[M+H]^+$, 1999 $[M+Na]^+$. Anal. Calcd for $C_{64}H_{68}Fe_2N_4O_{12}Pt_4$: C 38.88, H 3.47, N 2.83. Found: C 39.01, H 3.41, N 2.83.

8e: *Ar* = $C_6H_3(CF_3)_2$-*3,5*. **8e** was generated in the form of an orange powder (81% yield), mp 260−264 (decomp.). ^1H NMR (400 MHz, $CDCl_3$, 30 °C, δ/ppm): 2.02 (s, 6H, $^{ax}CH_3CO_2$), 2.04 (s, 6H, $^{ax}CH_3CO_2$), 3.95 (s, 10H, Cp H), 4.26 (t, $^3J_{HH}$ = 2 Hz, 4H, $-C_5H_4$), 4.46 (t, $^3J_{HH}$ = 2 Hz, 4H, $-C_5H_4$), 7.05 (s, 2H, −NCHN−), 7.79 (br s, 4H, $-C_6H_3(CF_3)_2$), 7.83 (s, 8H, $-C_6H_3(CF_3)_2$). $^{13}C\{^1H\}$ NMR (100 MHz, $CDCl_3$, 30 °C, δ/ppm): 21.6, 21.7 (s, $^{ax}CH_3CO_2$), 69.8 (s, Cp C), 70.6, 71.1, 71.6 (s, $-C_5H_4$), 118.0 (sept like, Ar C), 123.5 (q, $^1J_{CF} = 2.7 \times 10^2$ Hz, $-CF_3$), 124.5 (br s, Ar C), 132.3 (q, $^2J_{CF}$ = 33 Hz, Ar C), 150.0 (s, Ar C), 162.8 (s, −NCHN−), 186.6 (s, $-OCOC_5H_4$), 192.7, 194.4 (s, $^{ax}CH_3CO_2$). ^{19}F NMR (376 MHz, $CDCl_3$, 30 °C, δ/ppm): −63.5 ($-C_6H_4CF_3$). MS (FAB^+): *m/z*: 2408 $[M]^+$. Anal. Calcd for $C_{64}H_{44}F_{24}Fe_2N_4O_{12}Pt_4$: C 31.91, H 1.84, N 2.33. Found: C 31.54, H 1.43, N 2.32.

8f: *Ar* = $C_6H_3(^tBu)_2$-*3,5*. **8f** was generated in the form of a reddish brown powder (55% yield), mp 196−201 °C (decomp.). ^1H NMR (400 MHz, $CDCl_3$, 30 °C, δ/ppm): 1.40 (s, 72H, $-C_6H_4(C(CH_3)_3)_2$), 1.90 (s, 6H, $^{ax}CH_3CO_2$), 2.06 (s, 6H, $^{ax}CH_3CO_2$), 4.00 (s, 10H, Cp H), 4.09 (t, $^3J_{HH}$ = 2 Hz, 4H, $-C_5H_4$), 4.32 (t, $^3J_{HH}$ = 2 Hz, 4H, $-C_5H_4$), 7.05 (br s, 2H, −NCHN−), 7.25 (d, $^4J_{HH}$ = 1.6 Hz, 8H, $-C_6H_3(C(CH_3)_3)_2$), 7.30 (br t, 4H, $-C_6H_3(C(CH_3)_3)_2$). $^{13}C\{^1H\}$ NMR (100 MHz, $CDCl_3$, 30 °C, δ/ppm): 21.6, 21.9 (s, $^{ax}CH_3CO_2$), 31.8 (s, $-C_6H_3(C(CH_3)_3)_2$), 34.9 (s, $-C_6H_3(C(CH_3)_3)_2$), 70.0 (s, Cp C), 70.1, 71.1, 72.9 (s, $-C_5H_4$), 118.2, 118.6, 149.4, 150.9 (s, Ar C), 162.4 (s, −NCHN−), 185.3 (s, $-OCOC_5H_4$), 191.4, 194.1 (s, $^{ax}CH_3CO_2$). MS (ESI positive, CH_3CN): *m/z*: 2314 $[M+H]^+$. Anal. Calcd for $C_{88}H_{116}Fe_2N_4O_{12}Pt_4 \cdot 2Et_2O$: C 46.83, H 5.57, N 2.28. Found: C 47.06, H 5.53, N 2.39.

Preparation of $[Pt_4(\mu\text{-}OCOCH_3)_4(\mu\text{-}OCOC_5H_4FeCp)_2(\kappa^4\text{-}N_4\text{-}DArBp)]$. ***9a***: *Ar* = C_6H_4OMe-*4*. To a solution of **4a** (105 mg, 0.0645 mmol) in $CHCl_3$ (5 mL) was added a solution of ferrocenecarboxylic acid (31.5 mg, 0.137 mmol, 2.1 equiv) in a mixture of $CHCl_3$ (5 mL) and methanol (10 mL). The reaction mixture was stirred for 7 h at ambient temperature under reduced pressure. The removal of all of the volatiles afforded solids, which were washed with a mixture of Et_2O (4 mL) and hexane (4 mL, three times), followed by washing with a mixture of CH_2Cl_2 (1 mL), Et_2O (4 mL), and hexane (4 mL). **9a** was obtained as an orange powder (105 mg, 83% yield), mp 214−216 °C (decomp.). ^1H NMR (300 MHz, $CDCl_3$, 35 °C, δ/ppm): 1.8−1.9 (m, 2H, $-CH_2CH_2CH_2-$), 1.86 (s, 6H, $^{ax}CH_3CO_2$), 2.10 (s, 6H, $^{ax}CH_3CO_2$), 3.0−3.2 (m, 4H, $-CH_2CH_2CH_2-$), 3.77 (s, 6H, $-C_6H_4OCH_3$), 4.12 (s, 10H, Cp H), 4.20 (t, $^3J_{HH}$ = 2 Hz, 4H, $-C_5H_4$), 4.74 (br q, 2H, $-C_5H_4$), 4.81 (br q, 2H, $-C_5H_4$), 6.72 (d, $^3J_{HH}$ = 9.0 Hz, 4H, $-C_6H_4OCH_3$), 6.97 (d, $^3J_{HH}$ = 9.0 Hz, 4H, $-C_6H_4OCH_3$), 7.0−7.1 (m, 2H, $-C_6H_5$), 7.2—7.3 (m, 8H, $-C_6H_5$). $^{13}C\{^1H\}$ NMR (75 MHz, $CDCl_3$, 35 °C, δ/ppm): 21.7_6, 21.7_8 (s, $^{ax}CH_3CO_2$), 33.0 (s, $-CH_2CH_2CH_2-$), 51.5 (s, $-CH_2CH_2CH_2-$), 55.3 (s, $-C_6H_3OCH_3$), 69.7 (s, Cp C), 69.9, 71.3_0, 71.3_3, 75.4 ($-C_5H_4$), 113.0, 127.7, 127.8_7, 127.9_0, 128.0, 128.4, 129.7, 134.6, 141.3, 155.6 (Ar C), 172.9 (−NCPhN−), 181.0 ($OCOC_5H_4$), 191.8_7, 191.9_1 ($^{ax}CH_3CO_2$). MS (ESI positive, CH_3CN): *m/z*: 1965 $[M+H]^+$, 1735 $[M-OCOFc]^+$. Anal. Calcd for $C_{61}H_{60}Fe_2N_4O_{14}Pt_4 \cdot CHCl_3$: C 35.72, H 2.95, N 2.69. Found: C 35.99, H 2.78, N 2.69.

Similar procedures were conducted for $[Pt_4(\mu\text{-}OCOCH_3)_4(\mu\text{-}OCOC_5H_4FeCp)_2(\kappa^4\text{-}N_4\text{-}DArBp)]$ where Ar = C_6H_4Me-4 (**9b**) and $C_6H_3(^tBu)_2$-3,5 (**9c**).

9b: *Ar* = C_6H_4Me-*4*. **9b** was generated in the form of a brown powder (74% yield), mp 217−221 °C (decomp.). ^1H NMR (400 MHz, $CDCl_3$, 30 °C, δ/ppm): 1.86 (br s, 8H, $^{ax}CH_3CO_2$ + $-CH_2CH_2CH_2-$), 2.10 (s, 6H, $^{ax}CH_3CO_2$), 2.26 (s, 6H, $-C_6H_4CH_3$) 3.0—3.2 (m, 4H, $-CH_2CH_2CH_2-$), 4.13 (s, 10H, Cp H), 4.20 (t, $^3J_{HH}$ = 2 Hz, 4H, $-C_5H_4$), 4.73 (br s, 2H, $-C_5H_4$), 4.79 (br s, 2H, $-C_5H_4$), 6.93 (d, $^3J_{HH}$ = 8.4 Hz, 4H, $-C_6H_4CH_3$), 6.97 (d, $^3J_{HH}$ = 8.4 Hz, 4H, $-C_6H_4CH_3$), 7.0—7.1 (m, 2H, $-C_6H_5$), 7.2—7.3 (m, 8H, $-C_6H_5$). $^{13}C\{^1H\}$ NMR (100 MHz, $CDCl_3$, 30 °C, δ/ppm): 21.2 (s, $-C_6H_3CH_3$), 21.8_1, 21.8_3 (s, $^{ax}CH_3CO_2$), 33.0 (s, $-CH_2CH_2CH_2-$), 51.4 (s, $-CH_2CH_2CH_2-$), 69.7 (s, Cp C), 69.9, 71.3_8, 71.4_0, 75.5 ($-C_5H_4$), 127.7, 127.8, 127.9, 128.0, 128.3, 128.5, 128.7, 132.3, 134.7, 145.4 (Ar C), 172.6 (−NCPhN−), 181.1 ($OCOC_5H_4$), 191.9, 192.0 ($^{ax}CH_3CO_2$). MS (ESI positive, CH_3CN): 1971 $[M+K]^+$, 1955 $[M+Na]^+$, 1932 $[M]^+$, 1703 $[M-OCOFc]^+$. Anal. Calcd for $C_{61}H_{60}Fe_2N_4O_{12}Pt_4$: C 37.90, H 3.13, N 2.90. Found: C 37.74, H 3.31, N 2.87.

9c: *Ar* = $C_6H_3(^tBu)_2$-*3,5*. **9c** is generated in the form of a reddish orange powder (81% yield), mp 203−207 °C (decomp.). ^1H NMR (400 MHz, $CDCl_3$, 30 °C, δ/ppm): 1.20 (s, 36H, $-C_6H_3(C(CH_3)_3)_2$), 1.8−1.9 (m, 2H, $-CH_2CH_2CH_2-$), 1.94 (s, 6H, $^{ax}CH_3CO_2$), 2.12 (s, 6H, $^{ax}CH_3CO_2$), 3.1−3.2 (m, 4H, $-CH_2CH_2CH_2-$), 4.03 (s, 10H, Cp H), 4.06 (br q, 2H, $-C_5H_4$), 4.13 (br q, 2H, $-C_5H_4$), 4.16—4.19 (m, 2H, $-C_5H_4$), 4.86—4.89 (m, 2H, $-C_5H_4$), 6.99 (t, $^4J_{HH}$ = 2 Hz, 2H, $-C_6H_4(C(CH_3)_3)_2$), 7.1−7.2 (m, 8H, $-C_6H_4(C(CH_3)_3)_2$ + $-C_6H_5$), 7.2−7.3 (m, 6H, $-C_6H_5$). $^{13}C\{^1H\}$ NMR (100 MHz, $CDCl_3$, 30 °C, δ/ppm): 21.5, 21.8 (s, $^{ax}CH_3CO_2$), 31.5 (s, $-C_6H_3(C(CH_3)_3)_2$), 33.3 (s, $-CH_2CH_2CH_2-$), 34.5 (s, $-C_6H_3(C(CH_3)_3)_2$), 51.7 (s, $-CH_2CH_2CH_2-$), 69.6, 69.8, 70.9, 72.1, 74.9 (s, $-C_5H_4$), 69.9 (s, Cp C), 116.6, 123.0, 127.2, 127.9, 128.1, 128.4, 134.8, 147.2, 149.4, (s, Ar

C), 172.5 (s, −NCPhN−), 180.9 (s, −$OCOC_5H_4$), 191.6, 191.7 (s, $^{ax}CH_3CO_2$). MS (ESI positive, CH_3CN): m/z: 2167 $[M+K]^+$, 2151 $[M+Na]^+$, 2128 $[M]^+$. Anal. Calcd for $C_{75}H_{88}Fe_2N_2O_{12}Pt_4$: C 42.30, H 4.17, N 2.63. Found: C 42.12, H 4.11, N 2.56.

X-ray Crystallographic Analysis. Suitable crystals of **6** (red, block), **8a** (red, block), **8e** (red, block), **8f** (red, block), and **9b** (orange, platelet), which were grown via the diffusion of hexane into the toluene solution for **6**, diffusion of diethylether into the chloroform solution for **8a**, and slow evaporation of the saturated diethylether solution for **8e**, **8f**, and **9b**, were mounted on the CryoLoop (Hampton ReseArCh Corp.) with a layer of mineral oil and placed in a nitrogen stream. Complexes **6**, **8a**, **8e**, and **9b** were measured with a RAXIS-RAPID Imaging Plate (Rigaku) equipped with a sealed-tube X-ray generator (50 kV, 40 mA), using graphite monochromated Mo Kα (0.71075 Å) radiation in a nitrogen stream at 113(1) K. Complex **8f** was measured with a Mercury system (Rigaku) that was equipped with a sealed-tube X-ray generator (40 kV, 100 mA), using graphite monochromated Mo Kα (0.71075 Å) radiation in a nitrogen stream at 113(1) K. The unit-cell parameters and the orientation matrix for data collection were determined using the least-squares refinement method, and the setting angles are listed in Table S1 in the Supporting Information. The structures of all complexes were solved by direct methods on SHELXL-97.[34] All structures were refined on F^2 via full-matrix least-squares methods, using SHELXL-97.[34] Measured nonequivalent reflections with $I > 2.0\sigma(I)$ were used for the structure determination. The unit cell of **9b** contains two independent molecules: the Δ-isomer and the Λ-isomer. The non-H atoms (except for C3, C6, C7, C10, C11, C14, C15, C16, C17, O1, and O3 in **6**, C66, C67, C68, C69, and O65 in **8e**, C55, C56, C57, C58, O2, N2, and N3 in **8f**, and C38, C39, C40, C41, C42, C123, C124, C125, C126, O25, O26, and O27 in **9b**) were refined anisotropically. The H atoms were included in the refinement on calculated positions riding on their carrier atoms. The function minimized was $[\Sigma w(F_o^2 - F_c^2)]$, with w being given by the expression

$$w = \frac{1}{\sigma^2(F_o^2) + (aP)^2 + bP}$$

where $P = (\max(F_o^2,0) + 2F_c^2)/3$, with $\sigma^2(F_o^2)$ being obtained from counting statistics. The functions R_1 and wR_2 were given as

$$R_1 = \frac{\sum\left||F_o| - |F_c|\right|}{\sum|F_o|}$$

and

$$wR_2 = \left[\frac{\Sigma w(F_o^2 - F_c^2)^2}{\Sigma(wF_o^4)}\right]^{1/2}$$

The ORTEP-3 program was used to draw the molecules.[35]

Electrochemical Measurements. The CV and DPV voltammograms were recorded using an electrochemical analyzer (Model 610D, ALS/CH Instruments) in a 0.1 M $[^nBu_4N][PF_6]$ solution in dichloromethane or a 0.1 M $[^nBu_4N][BAr^F{}_4]$ solution in dichloromethane with a glassy carbon working electrode (GCE), a platinum wire auxiliary electrode, a saturated calomel reference electrode (SCE), and a scan rate of 100 mV/s (CV) or pulse amplitude of 50 mV (DPV). For the DPV voltammograms, the increment was 4 mV, the pulse width was 0.2 s, the sample width was 0.0167 s, and the pulse period was 0.5 s. Ferrocene was used as an internal reference. $[^nBu_4N][BAr^F{}_4]$ was prepared from $Na[BAr^F{}_4]$[36] via a salt metathesis reaction with $[^nBu_4N]Cl$.

■ ASSOCIATED CONTENT

Supporting Information. X-ray crystallographic data in CIF format for **6**, **8a**, **8e**, **8f**, and **9b**; synthesis and characterization of ArNHCHNAr (Ar = $C_6H_4Me_2$-3,5, $C_6H_4(CF_3)_2$-3,5, $C_6H_4(^tBu)_2$-3,5), H_2DArBp (Ar = $C_6H_3(^tBu)_2$-3,5), and $[Pt_4(\mu$-$OCOCH_3)_6(\kappa^4$-N_4-DArBp)] (Ar = $C_6H_3(^tBu)_2$-3,5 (**4c**)); molecular structure of **8e** and **8f** and tables of crystal data and refinement parameters for **6**, **8a**, **8e**, **8f**, and **9b**. These materials are available free of charge via the Internet at http://pubs.acs.org.

■ AUTHOR INFORMATION

Corresponding Author

*E-mail: mashima@chem.es.osaka-u.ac.jp.

■ ACKNOWLEDGMENT

This work was supported by a Grant-in-Aid for Scientific Research on Innovative Areas, "Molecular Activation Directed toward Straightforward Synthesis", from the Ministry of Education, Culture, Sports, Science and Technology, Japan, and CREST, JST. S.T. is thankful for the Grobal-COE Program of Osaka University. We appreciate Prof. Dr. T. Wada, Dr. H. Ohtsu, and Prof. Dr. K. Tanaka for electrochemical measurements. We also appreciate Prof. Dr. H. Tsurugi for his fruitful discussions and comments.

■ REFERENCES

(1) Braunstein, P.; Oro, L. A.; Raithby, P. R. *Metal Clusters in Chemistry*: Wiley−VCH: Weinheim, Germany, 1999.
(2) Bagai, R.; Christou, G. *Chem. Soc. Rev.* **2009**, *38*, 1011–1026.
(3) Venkateswara Rao, P.; Holm, R. H. *Chem. Rev.* **2004**, *104*, 527–559.
(4) Adams, R. D. *J. Organomet. Chem.* **2000**, *600*, l–6.
(5) Suzuki, H. *Eur. J. Inorg. Chem.* **2002**, 1009–1023.
(6) Harvey, P. D.; Mugnier, Y.; Lucas, D.; Evrard, D.; Lemaitre, F.; Vallat, A. *J. Cluster Sci.* **2004**, *15*, 63–90.
(7) Sculfort, S.; Braunstein, P. *Chem. Soc. Rev.* **2011**, *40*, 2741–2760.
(8) Low, P. J.; Brown, N. J. *J. Cluster Sci.* **2010**, *21*, 235–278.
(9) Zhu, N.; Pebler, J.; Vahrenkamp, H. *Angew. Chem., Int. Ed. Engl.* **1996**, *35*, 894–895.
(10) (a) Sasaki, Y.; Abe, M. *Chem. Rec.* **2004**, *4*, 279–290. (b) Tanaka, M.; Kariya, N.; Abe, M.; Sasaki, Y. *Bull. Chem. Soc. Jpn.* **2007**, *80*, 192–194.
(11) Geiger, W. E. *Organometallics* **2007**, *26*, 5738–5765.
(12) Cowan, D. O.; LeVanda, C.; Park, J.; Kaufman, F. *Acc. Chem. Res.* **1973**, *6*, 1–7.
(13) (a) Koridze, A. A.; Yanovsky, A. I.; Struchkov, Y. T. *J. Organomet. Chem.* **1992**, *441*, 277–284. (b) Cullen, W. R.; Rettig, S. J.; Zheng, T. C. *Polyhedron* **1995**, *14*, 2653–2661. (c) Lee, S.-M.; Cheung, K.-K.; Wong, W.-T. *J. Organomet. Chem.* **1996**, *506*, 77–84. (d) McAdam, C. J.; Duffy, N. W.; Robinson, B. H.; Simpson, J. *Organometallics* **1996**, *15*, 3935–3943. (e) Bruce, M. L.; Skelton, B. W.; Smith, M. E.; White, A. H. *Aust. J. Chem.* **1999**, *52*, 431–435. (f) Champeil, E.; Draper, S. M. *J. Chem. Soc., Dalton Trans.* **2001**, 1440–1447. (g) Bruce, M. I.; Skelton, B. W.; White, A. H.; Zaitseva, N. N *J. Organomet. Chem.* **2002**, *650*, 188–197. (h) Adams, R. D.; Qu, B.; Smith, M. D.; Albright, T. A. *Organometallics* **2002**, *21*, 2970–2978. (i) Adams, R. D.; Qu, B.; Smith, M. D. *Organometallics* **2002**, *21*, 3867–3872. (j) Albinati, A.; de Biani, F. F.; Leoni, P.; Marchetti, L.; Pasquali, M.; Rizzato, S.; Zanello, P. *Angew. Chem., Int. Ed.* **2005**, *44*, 5701–5705.
(14) (a) Churchill, M. R.; Li, Y.-J.; Nalewajek, D.; Schaber, P. M.; Dorfman, J. *Inorg. Chem.* **1985**, *24*, 2684–2687. (b) Cotton, F. A.; Falvello, L. R.; Reid, A. H., Jr.; Tocher, J. H. *J. Organomet. Chem.* **1987**, *319*, 87–97. (c) Costa, R.; López, C.; Molins, E.; Espinosa, E. *Inorg.*

Chem. **1998**, *37*, 5686–5689. (d) Cooke, M. W.; Murphy, C. A.; Cameron, T. S.; Swarts, J. C.; Aquino, M. A. S. *Inorg. Chem. Commun.* **2000**, *3*, 721–725. (e) Cooke, M. W.; T. Cameron, T. S.; Robertson, K. N.; Swarts, J. C.; Aquino, M. A. S. *Organometallics* **2002**, *21*, 5962–5971. (f) Boyd, D. A.; Crutchley, R. J.; Fanwick, P. E.; Ren, T. *Inorg. Chem.* **2010**, *49*, 1322–1324. (g) Boyd, D. A.; Cao, Z.; Song, Y.; Wang, T. W.; Fanwick, P. E.; Crutchley, R. J.; Ren, T. *Inorg. Chem.* **2010**, *49*, 11525–11531.

(15) (a) Chen, W.-Z.; Ren, T. *Organometallics* **2005**, *24*, 2660–2669. (b) Brown, D. J.; Chisholm, M. H.; Gallucci, J. C. *Dalton Trans.* **2008**, 1615–1624.

(16) (a) Xue, W.-M.; Kühn, F. E.; Herdtweck, E.; Li, Q. *Eur. J. Inorg. Chem.* **2001**, 213–221. (b) Xu, G.-L.; DeRosa, M. C.; Crutchley, R. J.; Ren, T. *J. Am. Chem. Soc.* **2004**, *126*, 3728–3729. (c) Berry, J. F.; Cotton, F. A.; Murillo, C. A. *Organometallics* **2004**, *23*, 2503–2506. (d) Kuo, C.-K.; Chang, J.-C.; Yeh, C.-Y.; Lee, G.-H.; Wang, C.-C.; Peng, S.-M. *Dalton Trans.* **2005**, 3696–3701. (e) Xu, G.-L.; Crutchley, R. J.; DeRosa, M. C.; Pan, Q.-J.; Zhang, H.-X.; Wang, X.; Ren, T. *J. Am. Chem. Soc.* **2005**, *127*, 13354–13363. (f) Xi, B.; Xu, G.-L.; Fanwick, P. E.; Ren, T. *Organometallics* **2009**, *28*, 2338–2341.

(17) (a) Chandrasekhar, V.; Nagendran, S.; Bansal, S.; Cordes, A. W.; Vij, A. *Organometallics* **2002**, *21*, 3297–3300. (b) Zheng, G.-L.; Ma, J.-F.; Su, Z.-M.; Yan, L.-K.; Yang, J.; Li, Y.-Y.; Liu, J.-F. *Angew. Chem., Int. Ed.* **2004**, *43*, 2409–2411.

(18) (a) Mereacre, V.; Nakano, M.; Gmez-Segura, J.; Imaz, I.; Sporer, C.; Wurst, C.; Veciana, J.; Turta, C.; Ruiz-Molina, D.; Jaitner, P. *Inorg. Chem.* **2006**, *45*, 10443–10445. (b) Ikegami, A.; Abe, M.; Inatomi, A.; Hisaeda, Y. *Chem.—Eur. J.* **2010**, *16*, 4438–4441.

(19) (a) Prokopuk, N.; Shriver, D. F. *Inorg. Chem.* **1997**, *36*, 5609–5613. (b) Kang, J.; Nelson, J. A.; Lu, M.; Xie, B.; Peng, Z.; Powell, D. R. *Inorg. Chem.* **2004**, *43*, 6408–6413. (c) Wei, Q.-H.; Zhang, L.-Y.; Shi, L.-W.; Chen, Z.-N. *Inorg. Chem. Commun.* **2004**, *7*, 286–288. (d) Wei, Q.-H.; Yin, G.-Q.; Zhang, L.-Y.; Chen, Z.-N. *Organometallics* **2006**, *25*, 4941–4944. (e) Koridze, A. A.; Sheloumov, A. M.; Dolgushin, F. M.; Ezernitskaya, M. G.; Rosenberg, E.; Sharmin, A.; Ravera, M. *Organometallics* **2008**, *27*, 6163–6169.

(20) Matsuzaka, H.; Qü, J.-P.; Ogino, T.; Nishio, M.; Nishibayashi, Y.; Ishii, Y.; Uemura, S.; Hidai, M. *J. Chem. Soc., Dalton Trans.* **1996**, 4307–4312.

(21) (a) Yip, J. H. K.; Wu, J.; Wong, K.-Y.; Yeung, K.-W.; Vittal, J. J. *Organometallics* **2002**, *21*, 1612–1621. (b) Yip, J. H. K.; Wu, J.; Wong, K.-Y.; Ho, K. P.; Pun, C. S.-N.; Vittal, J. J. *Organometallics* **2002**, *21*, 5292–5300.

(22) Stephenson, T. A.; Morehouse, S. M.; Powell, A. R.; Hefer, J. P.; Wilkinson, G. *J. Chem. Soc., Chem. Commun.* **1965**, 3632–3640.

(23) (a) Carrondo, M. A. A. F. de C. T.; Skapski, A. C. *J. Chem. Soc., Chem. Commun.* **1976**, 410–411. (b) Carrondo, M. A. A. F. de C. T.; Skapski, A. C. *Acta Crystallogr., Sect. B: Struct. Crystallogr. Cryst. Chem.* **1978**, *B34*, 1857–1862. (c) Carrondo, M. A. A. F. de C. T.; Skapski, A. C. *Acta Crystallogr., Sect. B: Struct. Crystallogr. Cryst. Chem.* **1978**, *B34*, 3576–3581.

(24) (a) Yamaguchi, T.; Sasaki, Y.; Nagasawa, A.; Ito, T.; Koga, N.; Morokuma, K. *Inorg. Chem.* **1989**, *28*, 4311–4312. (b) Yamaguchi, T.; Sasaki, Y.; Ito, T. *J. Am. Chem. Soc.* **1990**, *112*, 4038–4040. (c) Yamaguchi, T.; Ueno, T.; Ito, T. *Inorg. Chem.* **1993**, *32*, 4996–4997. (d) Yamaguchi, T.; Abe, K.; Ito, T. *Inorg. Chem.* **1994**, *33*, 2689–2691. (e) Yamaguchi, T.; Shibata, A.; Ito, T. *J. Chem. Soc., Dalton Trans.* **1996**, 4031–4032. (f) Shibata, A.; Yamaguchi, T.; Ito, T. *Inorg. Chim. Acta* **1997**, *256*, 179–204. (g) Yamaguchi, T.; Saito, H.; Maki, T.; Ito, T. *J. Am. Chem. Soc.* **1999**, *121*, 10738–10742. (h) Yamaguchi, T.; Shibata, A.; Ito, T. *Chem.—Eur. J.* **2001**, *7*, 5409–5418.

(25) (a) Ohashi, M.; Yagyu, A.; Yamagata, T.; Mashima, K. *Chem. Commun.* **2007**, 3103–3105. (b) Tanaka, S.; Yagyu, A.; Kikugawa, M.; Ohashi, M.; Yamagata, T.; Mashima, K. *Chem.—Eur. J.* **2011**, *17*, 3693–3709.

(26) (a) Abuhijleh, A. L.; Woods, C. *J. Chem. Soc., Dalton Trans.* **1992**, 1249–1252. (b) Christie, S. D.; Subramaniama, S.; Thompson, L. K.; Zaworotko, M. J. *J. Chem. Soc., Chem. Commun.* **1994**, 2563–2564. (c) Abuhijleh, A. L.; Pollitte, J.; Woods, C. *Inorg. Chim. Acta* **1994**, *215*, 131–137.

(27) Richardson, D. E.; Taube, H. *Inorg. Chem.* **1981**, *20*, 1278–1285.

(28) (a) Auger, A.; Swarts, J. C. *Organometallics* **2007**, *26*, 102–109. (b) Auger, A.; Muller, A. J.; Swarts, J. C. *Dalton Trans.* **2007**, 3623–3633.

(29) (a) Diallo, A. K.; Daran, J.-C.; Varret, F.; Ruiz, J.; Astruc, D. *Angew. Chem., Int. Ed.* **2009**, *48*, 3141–3145. (b) Diallo, A. K.; Absalon, C.; Ruiz, J.; Astruc, D. *J. Am. Chem. Soc.* **2011**, *133*, 629–641.

(30) Donoli, A.; Bisello, A; Cardena, R.; Benetollo, F.; Ceccon, A.; Santi, S. *Organometallics* **2011**, *30*, 1116–1121.

(31) Geiger, W. E.; Barriere, F. *Acc. Chem. Res.* **2010**, *43*, 1030–1039.

(32) (a) Barriere, F.; Camire, N.; Geiger, W. E.; Mueller-Westerhoff, U. T.; Sanders, R. *J. Am. Chem. Soc.* **2002**, *124*, 7262–7263. (b) Barriere, F.; Geiger, W. E. *J. Am. Chem. Soc.* **2006**, *128*, 3980–3989.

(33) Lin, C.; Protasiewicz, J. D.; Smith, E. T.; Ren, T. *Inorg. Chem.* **1996**, *35*, 6422–6428.

(34) Sheldrick, G. M. *Programs for Crystal Structure Analysis (Release 97-2)*; University of Göttingen: Göttingen, Germany, 1997.

(35) Farrugia, L. J. *J. Appl. Crystallogr.* **1997**, *30*, 565.

(36) Brookhart, M.; Grant, B.; Volpe, A. F., Jr. *Organometallics* **1992**, *11*, 3920–3922.